Numerical Simulation of Natural Convection between Two Immiscible Fluids in Channel Flow

Anil B Wakale

A Dissertation Submitted to
Indian Institute of Technology Hyderabad
In Partial Fulfillment of the Requirements for
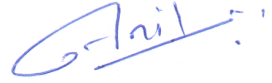The Degree of Master of Technology

भारतीय प्रौद्योगिकी संस्थान हैदराबाद
Indian Institute of Technology Hyderabad

Department of Mechanical and Aerospace Engineering

July 2014

Declaration

I declare that this written submission represents my ideas in my own words, and where ideas or words of others have been included, I have adequately cited and referenced the original sources. I also declare that I have adhered to all principles of academic honesty and integrity and have not misrepresented or fabricated or falsified any idea/data/fact/source in my submission. I understand that any violation of the above will be a cause for disciplinary action by the Institute and can also evoke penal action from the sources that have thus not been properly cited, or from whom proper permission has not been taken when needed.

(Signature)

Anil B Wakale
ME12M14P000003
(Roll No.)

Approval Sheet

This Thesis entitled Numerical Simulation of Natural Convection between Two Immiscible Fluids in Channel Flow by Anil B Wakale is approved for the degree of Master of Technology from IIT Hyderabad
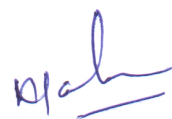
(Dr. Janardhanan Vinod) Examiner
Dept. of Chemical Eng
IITH

(Dr. Pankaj Kolhe) Examiner
Dept. of Mechanical And Aerospace Eng
IITH

(Dr. K.Venktasubbaiah) Adviser
Dept. of Mechanical And Aerospace Eng
IITH

(Dr. Sahu Kirti Chandra) Co-Adviser
Dept. of Chemical Eng
IITH

(Dr. Janardhanan Vinod) Chairman
Dept. of Chemical Eng
IITH

Acknowledgements

Dedication

Dedicated to my beloved parents and family...

Abstract

The buoyancy-driven interpenetration of two immiscible fluids in a differentially heated inclined channel is investigated by solving the Navier-Stokes, the continuity and the energy equations along with CahnHillard equation to track the interface. Fluids are separated by a partition and suddenly allowed to mix under the action of gravitational force. The governing equations are solved on staggered grid finite volume approach with second order accuracy in time integration. A parametric study is conducted to investigate the effects of Reynolds number, Bond number, Marangoni number, density ratio, viscosity ratio and temperature difference between the walls (ΔT) on flow dynamics of interface instability between two immiscible fluids. Results shows that increasing Reynolds number, Bond number, (ΔT) , density ratio and decreasing viscosity ratio destabilizes the flow dynamics by increasing the intensity of vortical structures and'mixing' of the fluids. The flow dynamics of vortical structures are altered by temperature gradient between the walls in comparison with isothermal system. The critical Bond number is identified as beyond which the flow dynamics becomes unstable leading to increasing the mixing of the fluids. The present results are matching well with the results available in the literature.

Contents

List of Figures

Chapter 1

Introduction

The interpenetration of two immiscible fluids in an confined inclined channel under the action of gravitational force is frequently encounter in many industrial and natural phenomena and thus has been investigated by several authors in the past research. Consider two immiscible fluids having different density and viscosity occupying the upper and lower half of an inclined channel and initially separated by a partition. At time, $t = 0$, the partition is suddenly removed and the fluids are allowed to mix by the action of the gravitational force. Several problem had been studied in past based on isothermal and non isothermal system with immisicible fluid in different types of geometry. The influence of combined buoyancy and thermal convection in immiscible liquid layers occurs in many industrial applications, such as alloying techniques, processing of ceramics and semiconductors that frequently involves molten and gaseous phases.

1.1   Litrature survey

In litrature survey analysis of two immiscible fluid had done by several anthers , e.g.[1, 2, 3, 4, 5, 6] This problem is frequently referred to as the "lock-exchange" problem [3, 7, 8, 9]. This phenomenon not only plays an important role in the design of chemical and petroleum engineering processes [1, 2], but also helps in understanding various natural systems in oceanography and atmospheric sciences [10].

   The "lock-exchange" problem Figure 2.1 has been investigated experimentally [3, 11, 12, 13, 14] and numerically [9, 5] by considering fluids having equal viscosity, although viscosity differential between fluids can have significant effect on the dynamics of the unsteady mixing process, which was recently investigated by Redapangu et al. [6]. The dimensionless parameters characterizing the flow in this problem are density contrast characterized by Atwood number, $At \equiv (\rho_1 - \rho_2)/(\rho_1 + \rho_2)$, the tilt angle, θ (measured from horizontal) and the viscosity ratio of the two fluids, $\mu_r (\equiv \mu_1/\mu_2)$, wherein ρ_1, μ_1 and ρ_2, μ_2 are the densities and viscosities of fluids '1' and '2', respectively. It is important to note here that all the above mentioned studies are for isothermal systems, although in most of the industrial applications this phenomena encounter with temperature gradient between the fluids and also in geometry having differentially heated boundaries. This is the subject of the present investigation. However, we shall discuss the dynamics associated with the isothermal systems first before discussing the previous works on non-isothermal systems.

1.1.1 Isothermal system

In isothermal "lock-exchange" flows [12], three types of flow regimes and mixing patterns were observed depending on the values of the tilt angle. In channel with tilt angles ($90° \geq \theta \geq 25°$), increasing θ decreases the magnitude of the front velocity of the high and low density fluids moving in the opposite directions. The front velocity (V_f) depends on the local density contrast across the interface. In this regime, flow and mixing are influenced by two distinct processes due to the components of the gravitational force along the axial and transverse directions of the channel. The former one accelerates the two fluids into each other at comparable velocities. During this motion, the interface separating the two fluids becomes unstable giving rise to the Kelvin-Helmholtz(KH) type instabilities, and consequent transverse mixing, which in turn decreases the front velocity. However, later one has an opposite effect by acting to segregate the two fluids and increases the front velocity. For lower tilt angles ($25° > \theta > 8°$) the front velocity is nearly constant, with a value approximately equals to $0.7\sqrt{Atgd}$, where g is the gravitational acceleration and d is a characteristic dimension (diameter of the pipe considered). For near horizontal channel ($\theta < 8°$) the flow transitions to a third regime where the two fluids move as counter-current Poiseuille flows; the front velocity increases with increasing the value of the tilt angle. In this regime, the flow dynamics is a result of the balance between buoyancy and wall friction. Hallez and Magnaudet [9] numerically studied the buoyancy-induced mixing of two fluids in circular, rectangular and square geometries, and found that the flow dynamics are more coherent and persistent in two than in three dimensions, which in turn give rise to more intense mixing and long-lasting flow structures in two-dimensional than in three dimensional geometries. Sahu and Vanka [5] investigated interpenetration of two immiscible fluids in a tilted channel using a lattice Boltzmann method (LBM). They conducted a parametric study by varying Atwood number, Reynolds number, tilt angle and surface tension. Their results compared well with the previous experimental results [3, 11, 12]. Meiburg and co-workers [15, 16] also studied the "lock-exchange" flows in the context of turbidity currents. Next we discuss the related works conducted on non-isothermal systems.

1.1.2 Non-isothermal systems

Several authors[17, 18, 19, 20, 21] investigated the effects the thermal convection in multiphase flows involving immiscible fluids by considering the temperature gradient along and normal to the interface. Prakash & Koster [17] studied thermal convection of two immiscible liquids in a container, which is differentially heated along the interface. They found that the flow pattern observed in their experiment agrees well with those obtained theoretically. Liu et al. [18] numerically studied the thermocapillary convection in a rectangular channel having temperature gradient normal to the interface of two immiscible liquids in the context of crystal growth. They found that the flow structure and temperature field are symmetric with respect to interface. It was concluded that by adjusting viscosity, conductivity of the fluids and thickness of the layers one could get desired flow patterns. Koster & Nguyen [22] showed that the appearance of two counter-rotating natural convection rolls in a system where the temperature at the left and right walls lie below and above the density inversion temperature, or vice-versa. The unsteady laminar natural convection with internal heat generation in rectangular container with water as a working fluid and temperature gradient along the interface is investigated by Hossain & Rees[21]. The top and bottom walls are

considered to be adiabatic. The effects of both heat generation and variations in the aspect ratio are investigated.

1.1.3 Miscible flow combination

Different type of studies have been conducted in miscible configurations such as displacement of one fluid by another fluid in channels,pipes,core-annular flows,hele-show cells and porous media. Experimentally studied density-driven instabilities between miscible fluids in a vertical Hele-Shaw cell,effect of tilt angle θ and differential viscous fluid combination reported in [23, 24]. The fluid having different density with more dense fluid is on top and less dense fluid on bottom subjected to gravitational force. The gravitational force have two component acts in axial and transverse direction which cause fluid to flow in channel. Increasing angle θ reduces transverse mixing of fluids. This is because buoyancy forces across the tube section stabilizing the interface between the fluids and reduces KelvinHelmholtz(KH) instabilities. In some of the stable system combination [25] gravity forces plays very important role in flow dynamics. They observed that when the gravity forces are neglected the flow dynamics does not depend on the direction of the displacement and when we consider the gravity effect interface becomes flat and finger like structures are formed at intermediate regime of channel. At this condition buoyancy and viscous forces are identical or balanced.

1.1.4 Immiscible flow combination

Sahu[26] Studied buoyancy induced in interpenetration of two immiscible fluids in tilted channel. The fluid is considered as incompressible and performed the analysis for isothermal system using lattice Boltzmann method (LBM). They observed when there is decrease in fluid viscosity it will increases Reynolds number and magnitude of front velocity. They studied the effect of parameters like Atwood number, Reynolds numbers, tilt angles and surface tension on flow dynamics between immiscible fluid.

Liu and Villers[18, 19] carried out experimental study on different fluid combination. In rectangular channel fluids are filled and side walls are heated at different temperature. Unrealistic fluid combination like having equal diffusivity and viscosity are considered. It shows flow structure and temperature field are symmetric in nature. (There will circulation from hot to cold wall and this is caused interfacial surface tension and temperature). Two dimensional laminar natural convection problem is studied in following work [20, 27, 28, 29]. The effect of instabilities is more when their is variation in density than viscosity. Linear stability analysis of two fluids which are initially motionless, viscous immiscible are confined between horizontal isothermal solid surfaces and subject to both density and surface-tension gradient(Marangoni)i.e. driving mechanisms is studied. It is found that flow and temperature field strongly depend upon internal heat generation parameter (absorption/generation) and wall temperature. When the fluids are heated from top, the buoyancy mechanism is stabilizing for most wave numbers, including the critical one. Heating from bottom leads to buoyancy driven flow for critical Marangoni number. when we consider density inversion condition deformation of the interface was not strongly affected by density inversion parameter (I), Rayleigh number(Ra), but it strongly affected by Marangoni effects (Ma), i.e., by thermocapillary driven-flow.

Redapangu et al.[30]studied the effects of viscosity differential on buoyancy-induced interpenetration of two immiscible fluids in a tilted channel using a two-phase lattice Boltzmann method implemented on a graphics processing unit. The effects of viscosity differential on the flow structures, average density profiles and front velocities are studied. Relatively stable fingers are observed for high viscosity ratios. The intensity of the interfacial instabilities and the transverse interpenetration of the fluids are seen to increase with decreasing viscosity differential of the fluids. The Navier Stokes and continuity equations coupled to two convective-diffusion equations for the concentration of both the scalars through concentration-dependent viscosity are solved using a finite-volume approach. Here The pressure-driven displacement of one fluid (initially filled inside a channel) by another (injected at the inlet) in a horizontal channel is studied. Both the fluids are the same, but consist of two scalars in different proportion[31].

1.2   Motivation

In spite of the large number of studies that investigated thermal convection, mixing and interpenetration of two immisicible fluids in a inclined channel with temperature gradient have not be investigated in literature. Also in most of the previous studies considered systems with stable temperature gradient such that the lighter fluid overlays the heavier fluid. Hence the present investigation has been motivated to understand the interface deformation for unstable system where a heavier fluid is overlying a lighter one in an inclined channel having differentially heated walls.

1.3   Objectives of present study

The objective of present study is to understand the interface deformation for unstable system where a heavier fluid is overlying a lighter one in an inclined channel having differentially heated walls. The problem statement of the current study is summarized as follows,

- To study the effect of interface instability between two immiscible fluids in a inclined channel.

- To study the effect of Reynolds number on interface instability.

- To study the effect of surface tension.

- To study the effect of viscosity ratios.

- To study the effect of surface tension variation with temperature and density ratios.

1.4   Outline of the thesis

In the present work , the numerical simulation of tow immiscible fluids is conducted using Finite volume method. The instability patterns arise in the flow due to gravity forces acting on channel i.e. in axial and in transverse direction. A brief background relevant application and a extensive literature survey on the problem considered and discussed in Chapter 1.

In Chapter 2, mathematical formulation of the current multiphase Finite volume method is formulated. All the governing equation which used in numerical simulation is studied. Numerical methodology used to solve the problem is discussed in this chapter.

The contours of Reynolds number, deferentially heated wall temperature, Bond number, viscosity, Marangoni number,and density variation of fluids are plotted of two dimensional channel in Chapter 3.

Finally, the whole study presented in summarised and concluded in Chapter 4.

Chapter 2

Governing equations and Numerical methods

Consider buoyancy-driven flow of two immiscible liquids in an inclined two-dimensional confined channel of length, L and height, H having differentially heated rigid and impermeable walls as shown in Figure 2.1 . The walls at $y = 0$ and $y = H$ are maintained at temperature T_h and T_c, respectively, and the walls at $x = (0, L)$ are adiabatic. The liquids are assumed to be Newtonain and incompressible. A rectangular coordinate system (x, y) to model the flow dynamics, where x and y denote the axial and transverse coordinates, respectively. The flow dynamics is governed by continuity, incompressible Navier-Stokes equations along with energy equation. The diffuse interface method [4] is used to track the interface separating the immiscible fluids; the Cahn-Hillard equation for the volume fraction of the lighter fluid, C is solved for this purpose.
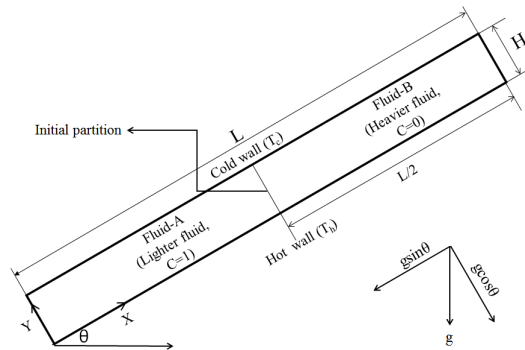

Figure 2.1: Schematic diagram presenting the initial equilibrium configuration. The aspect ratio of the channel is 1 : 40.

2.1 Governing equations

2.1.1 Continuity and CahnHilliard equations

It is assumed as unsteady two dimensional incompressible laminar flow between immiscible fluids (A and B) with different density and viscosity. Similar to the VOF method, the volume fraction of one of the fluids is used to indicate the composition of the two components in a volume element in the domain. If the volume fraction of component A is denoted by C ($0 \leq C \leq 1$) (we have consider as 0 can be taken for heavier fluid and 1 for the lighter fluid),the local averaged density,viscosity and thermal conductivity values given by,

$$\rho = C\rho_A + (1 - C)\rho_B$$
$$\mu = C\mu_A + (1 - C)\mu_B$$
$$K = CK_A + (1 - C)K_B$$

In this case, when an amount of fluid A flows out of an interface volume element due to interfacial diffusion, there will also be an amount of fluid B of the same volume that would enter the volume element at the same time, and vice versa. It can be given by $j_B = -j_A$ so the the volume diffusive flux of the two species are of equal magnitude, but of opposite sign. It is therefore convenient to introduce the notation $j = j_A$ and $j = -j_B$.

The continuity equation given by,

$$\nabla \cdot u = 0 \tag{2.1}$$

Convective CahnHilliard equation for volume fraction given by,

$$\frac{\partial C}{\partial t} + u \cdot \nabla C - \nabla \cdot j = 0 \tag{2.2}$$

2.1.2 Momentum equation

The Navier Stokes equation,

$$\rho(\frac{\partial u}{\partial t} + u \cdot \nabla u) = -\nabla p + \nabla \cdot (\mu(\nabla u + \nabla u^T)) + F \tag{2.3}$$

In above equations, $u = (u, v)$ denotes the velocity field in which u and v represent the axial and transverse velocity components, respectively, p is the pressure field, t denotes time, and F is the combined body and surface forces per unit volume, which include the gravity and surface tension forces given by,

$$F = \frac{\phi \nabla C}{Bo}(1 - \mathcal{M}T) - \rho\vec{j}, \tag{2.4}$$

where $\vec{j}$ represents the vertical direction, ϕ is chemical potential, given by $\epsilon^{-1}\sigma\alpha\psi'C - \epsilon\sigma\alpha\Delta C$, wherein $\psi(C) = C^2(1 - C^2)/4$ is the bulk energy density, σ is the coefficient of surface tension, and ϵ is the measure of interface thickness, α is a constant [32]. This momentum balance has been widely used in DI models. An attempt to combine a rough approach for the derivation of the CahnHilliard equation for solenoidal velocity fields with that of the Navier Stokes equations has been presented by Boyer, but it involves several approximations for a specific flow configuration.

2.1.3 Energy equation

$$\rho C_p \left(\frac{\partial T}{\partial t} + u \cdot \nabla T \right) = \nabla \cdot (K \nabla T) \tag{2.5}$$

Using Boussinesq approximation β_A and β_B are defined as,

$$\beta_{(A,B)} = -\frac{1}{\rho_{(A,B)}} \left(\frac{\partial \rho_{(A,B)}}{\partial T} \right)_p \tag{2.6}$$

Now by varying the density of two fluids and the temperature difference at end wall, we will get averaged density,viscosity and thermal conductivity of two fluids given by,

$$\rho^* = C(1 - \beta_1 \Delta T) + (1 - C)\rho_r(1 - \beta_2 \Delta T) \tag{2.7}$$

$$\mu^* = (C + (1 - C)\mu_r)e^{-T} \tag{2.8}$$

$$K^* = C + (1 - C)r_k \tag{2.9}$$

Where ρ_r density ratio $\frac{\rho_B}{\rho_A}$, μ_r is viscosity ratio $\frac{\mu_B}{\mu_A}$ and r_k conductivity ratio $\frac{k_B}{k_A}$.

Following scales are used to nondimensionalize the governing equations,

$X^* = \frac{x}{L}$, $\quad Y^* = \frac{y}{L}$, $\quad U^* = \frac{u}{U}$, $\quad V^* = \frac{v}{U}$, $\quad P^* = \frac{p}{\rho_A u^2}$, $\quad \mu^* = \frac{\mu}{\mu_A}$,

$T = T^*(T_h - T_c) + T_c$

where the tildes removed from dimensionless quantities,T_h and T_c are the temperatures of the hot and cold walls, respectively; U is the characteristic velocity, given by $\sqrt{gH}$; g being the acceleration due to gravity, μ_A, ρ_A and K_A are the viscosity, the density and the thermal conductivity of fluid A (lighter fluid) at the reference temperature, T_c respectively.

2.2 Non-dimensionalized form of equations

Continuity equation

$$\nabla \cdot u = 0 \tag{2.10}$$

Volume fraction equation

$$\frac{\partial C}{\partial t} + (u \cdot \nabla)C = \frac{1}{Pe} \nabla \cdot (M \nabla \phi) \tag{2.11}$$

Momentum equation

$$\rho \left(\frac{\partial u}{\partial t} + u \cdot \nabla u \right) = -\nabla p + \frac{1}{Re} \nabla \cdot (\mu(\nabla u + \nabla u^T)) + \frac{\rho}{Fr^2} + \frac{\phi \Delta C}{B_0} \tag{2.12}$$

Energy equation

$$\frac{\partial T}{\partial t} + u \cdot \nabla T = \frac{1}{RePr} \nabla \cdot (K \nabla T) \tag{2.13}$$

Definitions and Concepts of dimensionless numbers

- Reynold number(Re)= The Reynolds number is defined as the ratio of inertial force to viscous force. It signifies whether the flow is laminar or turbulent.

  Reynold number$(Re) = \frac{\rho U H}{\mu}$ Where, Velocity (U)= $\sqrt{gH}$

- Peclet number(Pe)= The peclet number is defined as the ratio of advective transport rate to the diffusive transfer rate. It shows the transport phenomena of fluid in flow.

  Peclet number $(Pe) = \frac{LU}{M_c \Phi_c}$ Where, M_c and Φ_c are characteristic values of mobility and chemical potential.

- Bond number(Bo)= The Bond number is a measure of the importance of surface tension forces compared to body forces.

  Bond number $(B_o) = \frac{\rho g L^2}{\sigma}$ Where, L is characterstic length and σ is the surface tension of the interface.

- Prandtl number(Pr)= Prandtl number is defined as the ratio of momentum diffusivity (kinematic viscosity) to thermal diffusivity.

  Prandtl number $(Pr) = \frac{\mu C_p}{K}$

- Froude number(Fr)= It is defined as the ratio of a characteristic velocity to a gravitational wave velocity. It can be defined as the ratio of a body inertia to gravitational forces.

  Froude number $(Fr) = \frac{U}{\sqrt{gH}}$

- Marangoni number (Ma)= The Marangoni effect (also called the Gibbs Marangoni effect) is the mass transfer along an interface between two fluids due to surface tension gradient.

  Marangoni$(Ma) = \frac{1}{\sigma_0} \frac{d\sigma}{dT}$

2.2.1   Initial condition and boundary

Initially at t=0, concentration of lighter fluid C=1, heavier fluid is C=0. Governing equations (2.10-2.13) are solved using no-slip and no-penetration boundary conditions at all the walls and the Neumann boundary conditions are imposed at the boundaries for concentration field. The walls at $y = 0$ and $y = 1$ are maintained at temperature T_h and T_c, respectively, and Neumann boundary conditions for temperature are used at the rest of the boundaries. The numerical method used in the present study is similar to the one of Ding et al. [4]. The reader is also referred to the supplementary material of for an extensive validation of the present code. In addition, we have ensured that convergence is indeed achieved upon mesh refinement.

2.3 Numerical method

A staggered grid finite-volume approach is incorporated in order to solve the system of equations (2.10)-(2.13). The scalar variables (the pressure and the volume fraction of the lighter fluid) are defined at the cell-centers and the velocity components are defined at at the cell faces, respectively. A weighted-essentially-non-oscillatory (WENO) scheme is used for discretization of the advective term in Eq. (2.12), and a central difference scheme is used to discretize the diffusive term. The Adams-Bashforth and the Crank-Nicholson methods are respectively used for the advective and second-order dissipation terms in Eq. (2.11) is used in order to achieve second-order accuracy in the temporal discretization. In the solver, the initial conditions are prescribed as discussed above. Then the Cahn-Hillard equation (Eq. (2.12)) is first solved and the concentration filed is updated using the velocity field at previous time-steps (n^{th} step). The velocity field is then updated to next time step ($(n+1)^{th}$ step) by solving Eq. (2.11) in conjunction with the continuity equation (Eq. (2.10)). This process is repeated as the time progress.
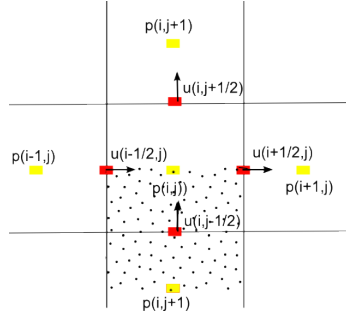

Figure 2.2: The schematic diagram of staggered grid

The time dependent non linear coupled partial differential equations were solved by considering a 701×41, 2001×121 and 2562×66 grid depending on the different values of aspect ratio. The convergence of the numerical solutions was verified by mesh refinement. In order to accurately describe gradients in boundary layers, a non uniform grid in both the x and y directions is used. There will following advantages to used finite volume method like

1. Numerical stability will be better it can take Δt longer steady state can reached faster.

2. For complex stability need j^{n+1} to get that we need all in one loop by making semi implicit as we can solve ω and Ψ in two seperate loops instead of solving both simultaneously in one loop.

In book of Oosthuizen [33] study numerical simulations of steady state free convection heat transfer in closed channel , totally filled with one liquid or gas. There will be different instabilities when channel field with one liquid or gas. Flow structure is different. Now when a channel contain gas the convective heat transfer rate can be low and radiant heat transfer may be significant but some gases absorb and emits radiation in such case energy equation has to be modified.

Chapter 3

Results and Discussion

Buoyancy-driven mixing of two immiscible fluids in a inclined heated channel is studied numerically. The heated wall is maintained at a constant surface temperature (T_h) and it is greater than the fluids temperatures. The top or bottom wall is considered as heated wall and side walls are insulated. We studied effects of various parameters like Reynolds number, wall temperature, surface tension, viscosity ratio, Marangoni number and density ratio on flow dynamics of interface instability.
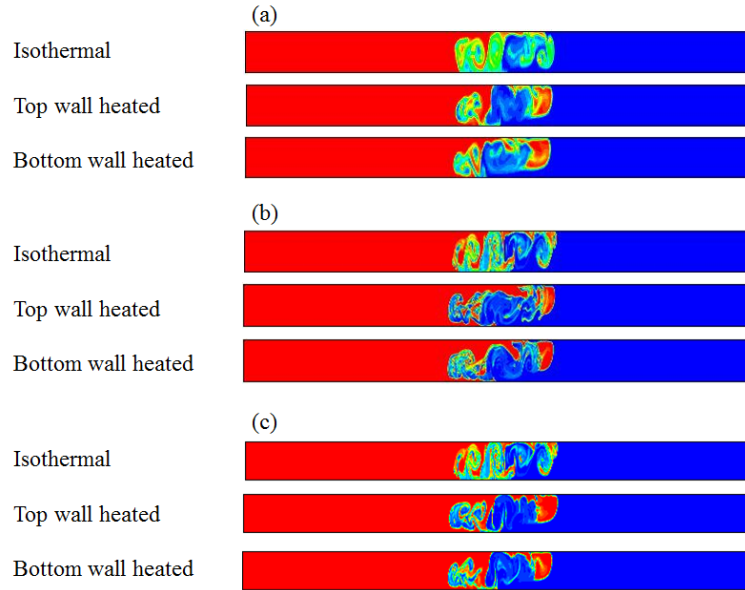
3.1   Grid independence test

Figure 3.1: The contours of the volume fraction C at t= 40 obtained using grids (a)701 × 41, (b)2001 × 121 and (c)2562 × 66.

The contours of the volume fraction of the lighter fluid, C for a typical set of parameters are plotted at t = 40 for different grids. It can be seen that the results for 2001×121 and 2562×66 are nearly the same. In view of this agreement obtained for the finer meshes, we opted to use 2562 and 66 grid points in the x and y directions, respectively for the rest of the calculations presented in this thesis.
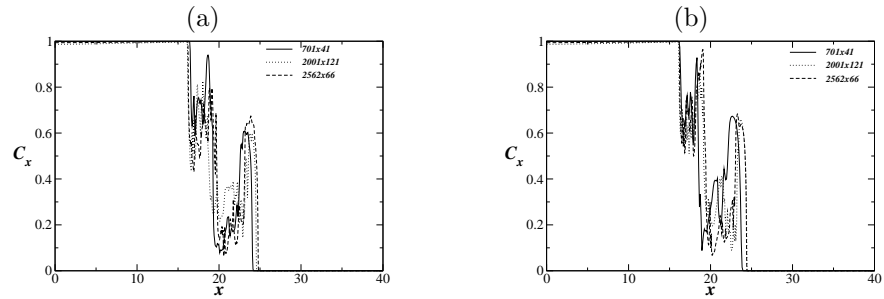

Figure 3.2: The axial variation C_x at t= 40 obtained using grids (a)701×41, (b)2001×121 and (c)2562×66. for (a)top wall heated case and (b)bottom wall heated case.

3.2 Effect of Reynolds number

We begin the presentation of our results obtained by studying the effects of Reynolds number. The spatio-temporal evaluations of the contours of the volume fraction of the lighter fluid, C are plotted for Re = 50, 100, 200 and 1000 are plotted in Fig. 3.3, 3.4 respectively. In each panel the results for heated top and bottom walls are plotted along with the isothermal case. It can be seen that due to the gravitational force acting in the axial direction, proportional to $gsin\theta$, of the finger of the heavier fluids penetrates into the region of the lighter fluid in the negative axial (x) direction. In order to satisfy the conservation of mass the lighter fluid then moves in the positive x direction into the region of the heavier fluid. This motion of the heavier and lighter in the opposite directions leads to the development of mixed type of Kelvin-Helmholtz (KH) and Rayleigh-Taylor (RT) instabilities, which in turn give rise to the vortical structures which enhance the interpenetration of the fluids. On the other hand, the fluids are segregated due to the gravitational force acting in the transverse direction, proportional to $gcos\theta$. Thus the resultant complex dynamics observed in this figure is due to the competition of the gravitational force acting in the axial and transverse directions.
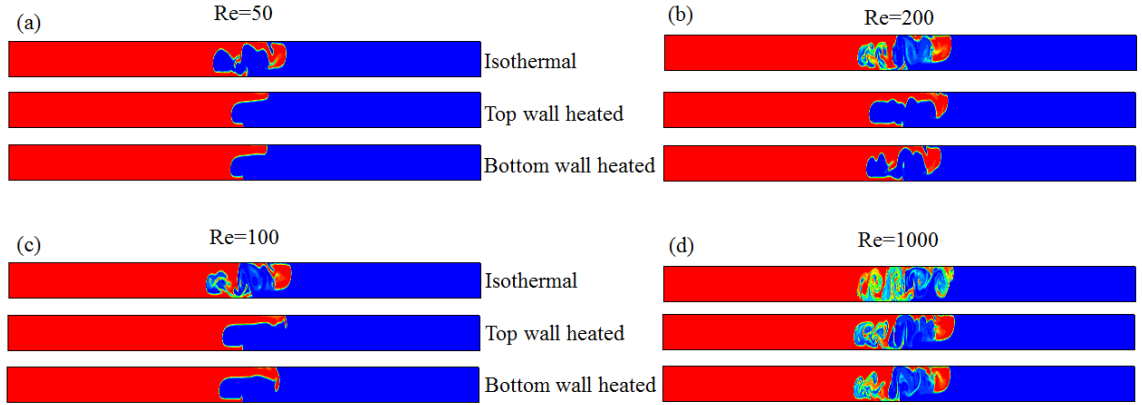

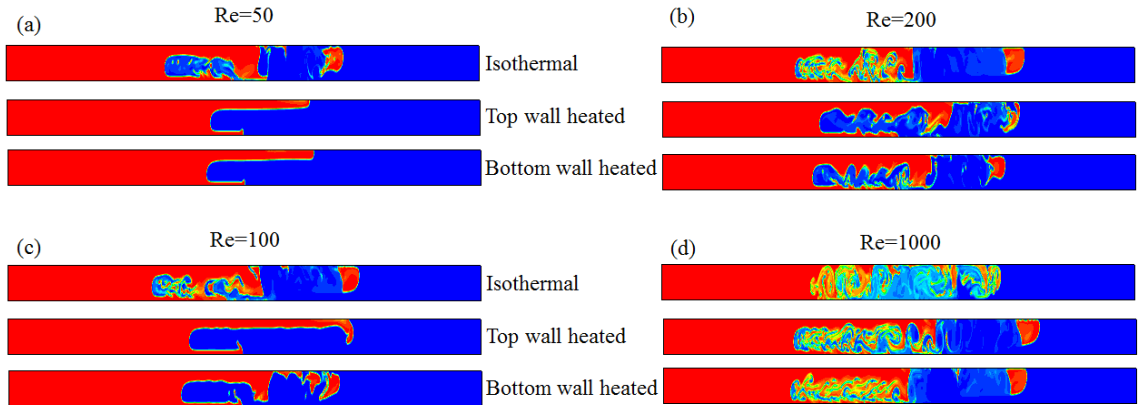Figure 3.3: Comparison of different Reynolds number at t=40.

Figure 3.4: Comparison of different Reynolds number obtained by finite volume(FV) method using 2562 and 66 grid points in x and y direction respectively, for channel of aspect ratio 1:40 at t=100.
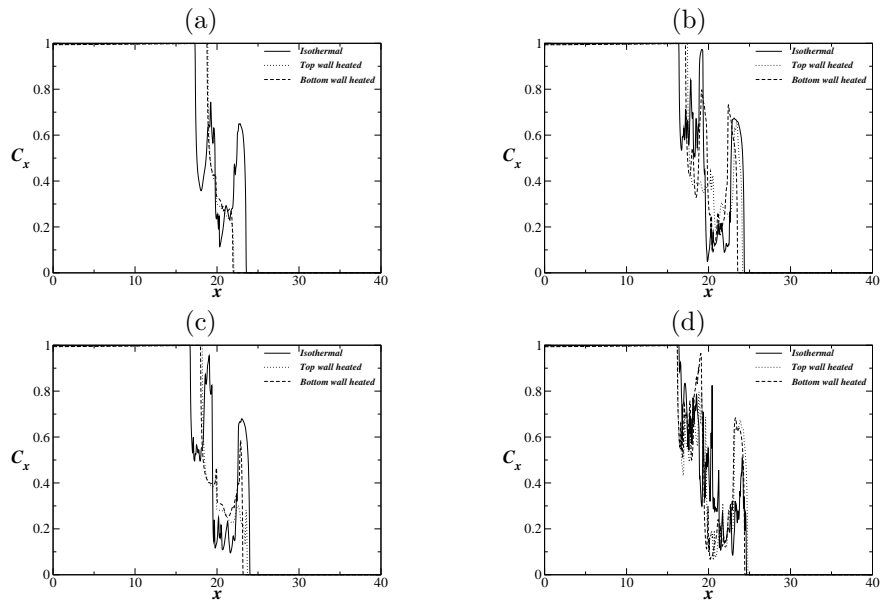
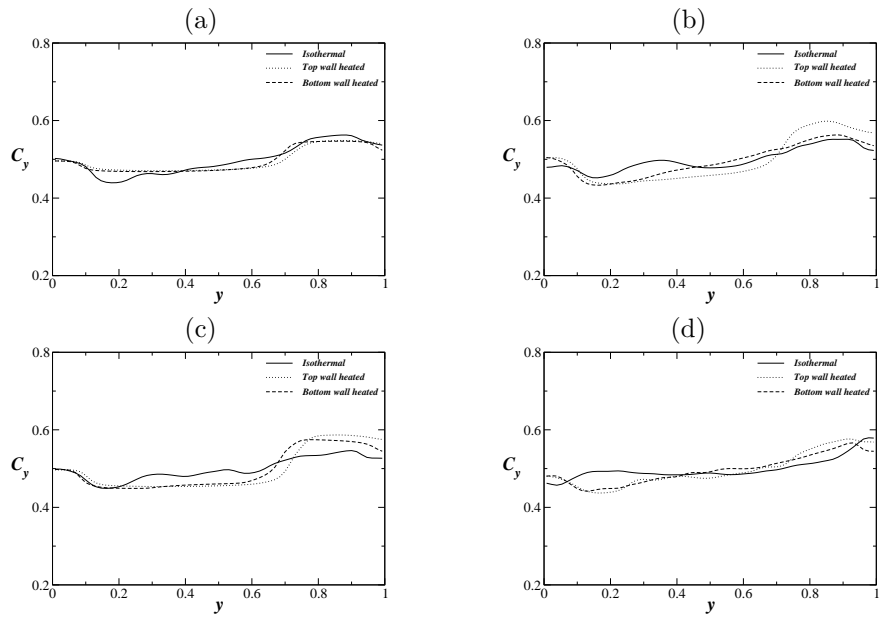Figure 3.5: Effect of Reynolds number on axial variation of depth-average C_x at t=40

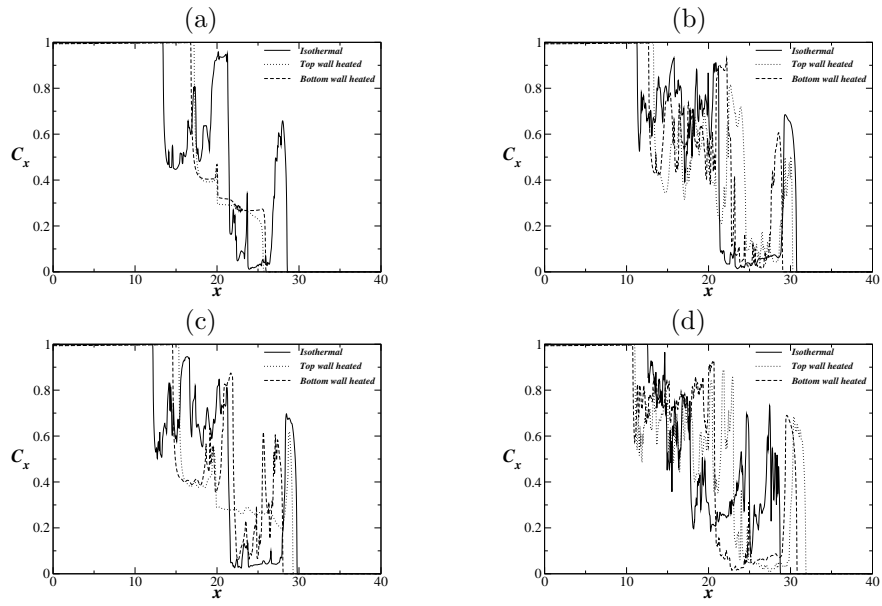Figure 3.6: Effect of Reynolds number on transverse variation of depth-average C_y at t=40

Figure 3.7: Effect of Reynolds number on axial variation of depth-average C_x at t=100 as (a,b,c,d) corresponds to Re=50,200,100,1000 respectively
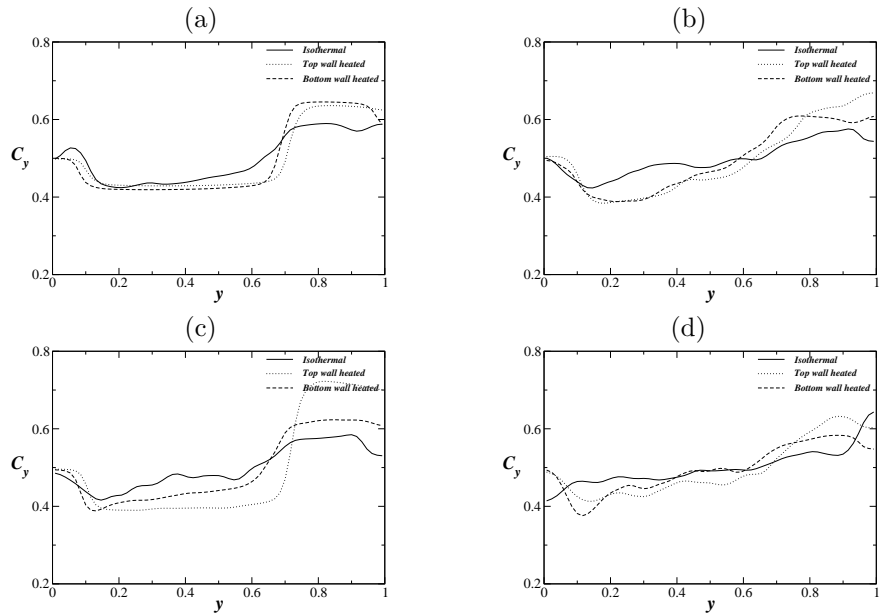

Figure 3.8: Effect of Reynolds number on transverse variation of depth-average C_y at t=100

Inspection of Fig. 3.3 reveals that the presence of heated wall, irrespective of the situations whether the top or bottom walls are heated, reduces the instabilities as compared to the isothermal case due to thermal convection. As expected, the comparison of the top and bottom wall heated cases shows that the flow dynamics is more unstable in case of bottom wall heated case. This is due to the fact that when the bottom wall is hotter than the top wall, the fluids near the bottom wall becomes lighter and moves in the upward direction due to the gravitational force, which enhance the interpenetration of the lighter fluid into the region of the heavier fluid in the transverse direction. It can also be seen that increasing Reynolds number increases the intensity of instabilities and small-scale structures, which in turn increases the 'mixing' of the fluids. Close inspection of Fig 3.5(a) also reveals that for lower value of Reynolds number at later times (see e.g. t = 100) Fig.3.7(a) the speed of the heavier fluid is slower than that of the lighter fluid. This effect is more prominent for the top wall heated case. However, for Re = 1000 the inertial effects is significant and the asymmetrical effect observed for Re = 100, which arises due to thermal convection is minimized.

The axial variation of average concentration C_x along the length of the channel is shown in Fig. [3.5-3.8] for Re = 50, 100, 200 and 1000. From these plots higher magnitude and more oscillations are observed in isothermal flows than non isothermal flows at Re = 100. The magnitude and spreading length increases with increase in Reynolds number. Higher magnitude and more oscillations are observed in non isothermal flows than isothermal flows at high Reynolds number Re = 1000.
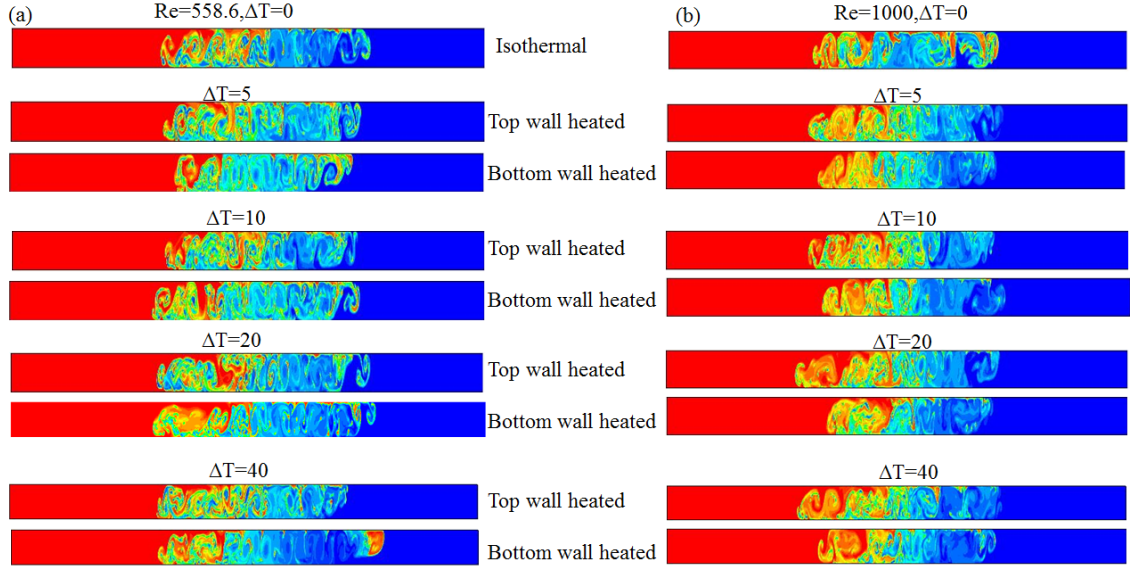
3.3   Effect of wall temperature

Figure 3.9: Comparison of wall temperature counters obtained by finite volume(FV) method using 2562 and 66 grid points in x and y direction respectively, for channel of aspect ratio 1:40 at t=100 as (a),(b) corresponds to Re=558.6, 1000 respectively
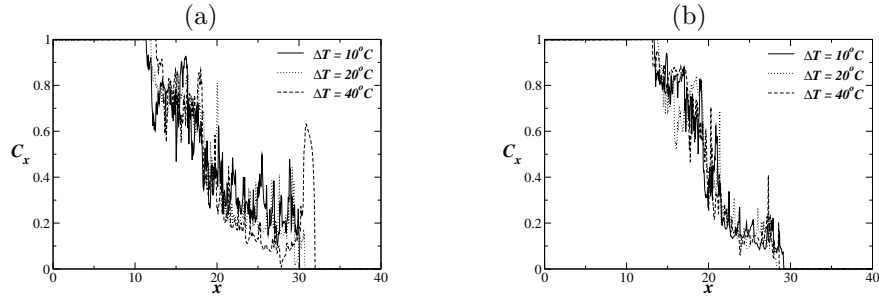
Figure 3.10:   Effect of wall temperature on axial variation of depth-average C_x at t=100 fig (a),(b)Re=558.6,1000 respectively

The counters shows that variation of wall temperature in Fig. 3.9 at t=100. It shows that instabilities were reducing as temperature increase and its more in bottom wall heated case at Re=1000. We studied convection at $\Delta T= 5,10,20$ and 40 at Re=558.6,1000. Fig. 3.10 shows axial variation of depth-average C_x at t=100, with $\Delta T=10,20$ and 40. More focus will be on Re=1000 and which discussed is further in brief below at different time steps.
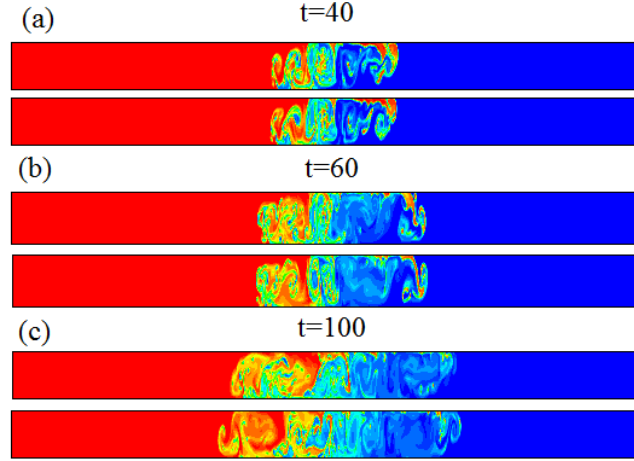
Figure 3.11: The spatio-temporal evaluation of contours of the volume fraction of the lighter fluid, C for different values wall temperature at (a) t = 40, (b) t = 60 and (c) t = 100
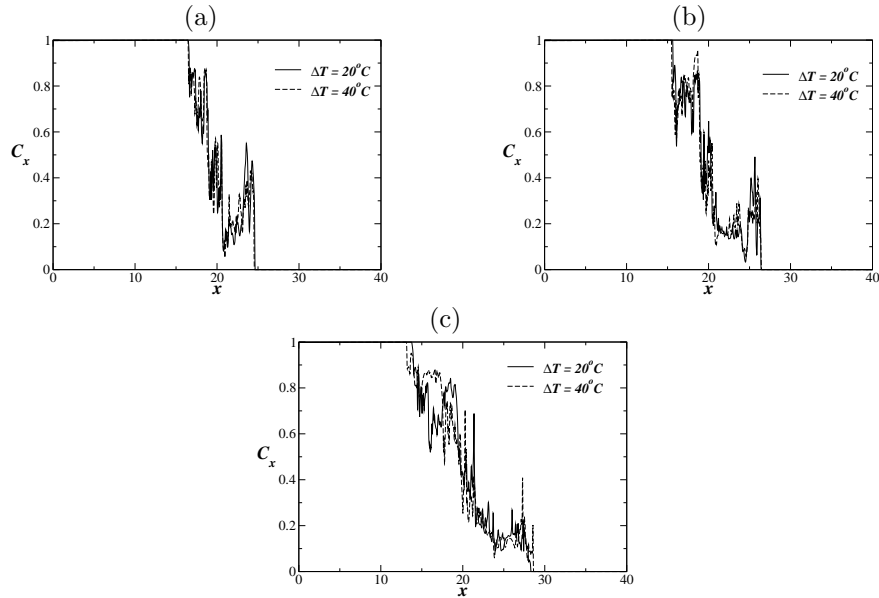
Figure 3.12: Effect of heated wall temperature at different time t=40,60,100 with bottom heating as (a),(b)and(c) at ΔT=20,40 respectively

As the thermal convection is more for bottom-wall heated case, we considered only this case to investigate the effects of temperature difference between the top and bottom walls $\Delta T = T_h - T_c$ The spatio-temporal evaluations of C are plotted for $K_{(A,B)}$ =0.2 and 0.4 which correspond to $\Delta T = 20^0$C and $\Delta T = 40^0$C for $\beta = 10^{-3}$. It can be seen that due to the increase in buoyancy force with the increase in the temperature gradient between the wall, the intensity of the interfacial instabilities increases. Close inspection of Fig. 3.11 also reveals that increasing ΔT(i.e increasing buoyancy) increases the axial velocity of the fingers. Thus axial spreading length increases with increasing ΔT. The axial variations of the transverse averaged volume fraction of the lighter fluid, C_x for different valus of ΔT are shown in Fig. 3.12 This plot shows that the spreading length increases with increasing in ΔT at every time.

3.4 Effect of surface tension

Figure 3.13: Comparison of different Bond number t=40

Figure 3.14: Comparison of different Bond number obtained by finite volume(FV) method using 2562 and 66 grid points in x and y direction respectively, for channel of aspect ratio 1:40 at t=100

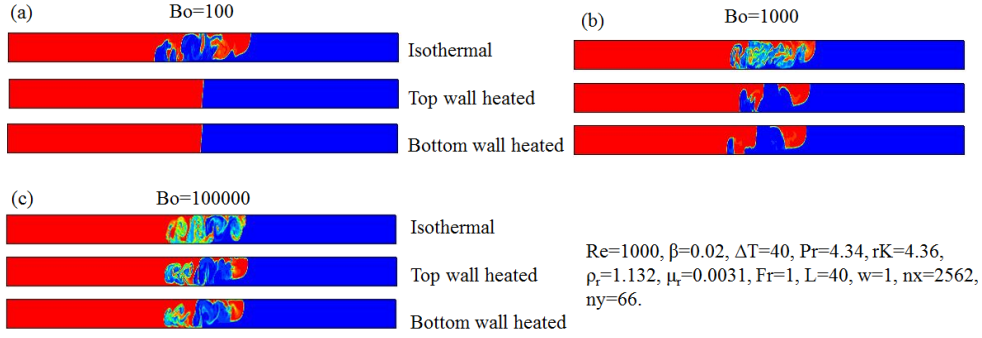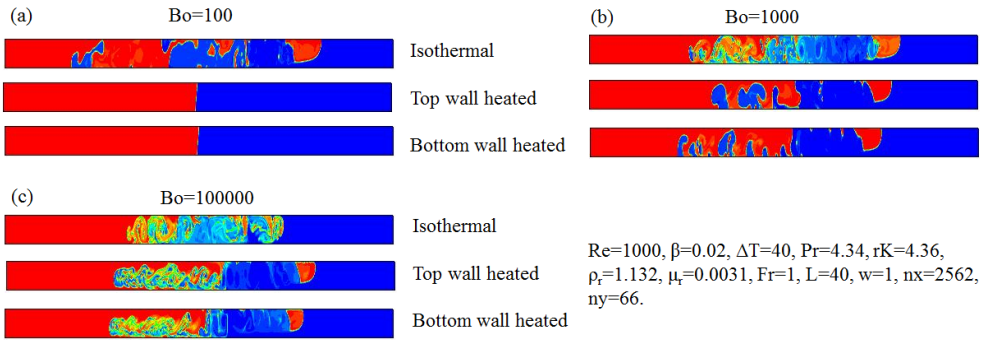We investigate the effect of surface tension in Fig. [3.13-3.14]as t=40,100 respectively, where the contours of the volume fraction of the lighter fluid, C are plotted for Bo = 100, 1000 and 100000 for isothermal, top-wall and bottom-wall heated cases. Increasing Bo means decreasing surface tension, if we keep the other scale same. Rest of the parameter value are Re=1000,M_a=0, P_r=7, $\theta = 60^0$,$K_r = 4.36$,rd=1.4,μ_r=0.0031. It can be seen that for both the values of Bo considered the flow dynamics is more stable in case of nonisothermal systems as compared to that of the isothermal system. This is due to the fact that surface tension opposes the effect created by the gravitational force in the axial direction. Like the gravitational force in the transverse direction, surface tension prevents the motion of the fingers in the opposite direction. It can be observed that the interface is almost stationary even at the later times for low value of Bo (high surface tension) considered. In this case the effects of surface tension and gravitational force in the transverse direction counterbalance with that of the axial component of the gravitational force. For Bo = 1000 (shown in Fig.3.14(b)) the effect of surface tension is less as compared to Bo = 100 case (shown in in Fig. 3.14(a)). Therefore although the interfacial instabilities appear, the intensity of these instabilities is much lower than those observed in case of isothermal case. Close inspection also reveals that for higher Bo the axial motion of the fingers becomes asymmetrical, and as the lighter fluid moves into the region of the heavier fluid, a blob of the lighter fluid detached from the main finger, which moves in the upward direction almost independently.

3.5 Effect of viscosity ratio

Figure 3.15: Comparison of different Viscosity ratio obtained by finite volume(FV) method using 2562 and 66 grid points in x and y direction respectively, for channel of aspect ratio 1:40 at t=100 where fig (a,c,e)at μ_r=0.01 and(b,d,f)at μ_r=0.1
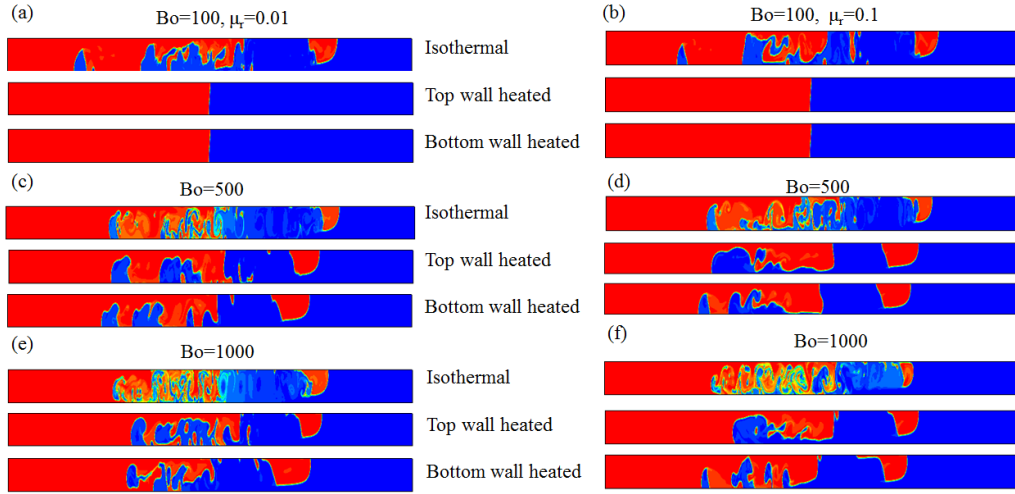

Figure 3.16: Comparison of different Viscosity ratio obtained by finite volume(FV) method using 2562 and 66 grid points in x and y direction respectively, for channel of aspect ratio 1:40 at t=100 where fig (a,c,e)at μ_r=1 and(b,d,f)at μ_r=10

The study was conducted based on different viscosity ratio as shown in counters [3.15-3.16] with varying Bond number. From counters it mainly shows that as we increased viscosity beyond 10 stability increased more in wall heated case. There will be different fluid velocity of lighter and heavier fluid. Stability is continuously increasing from μ_r=0.01, 0.1, 1 and 10.
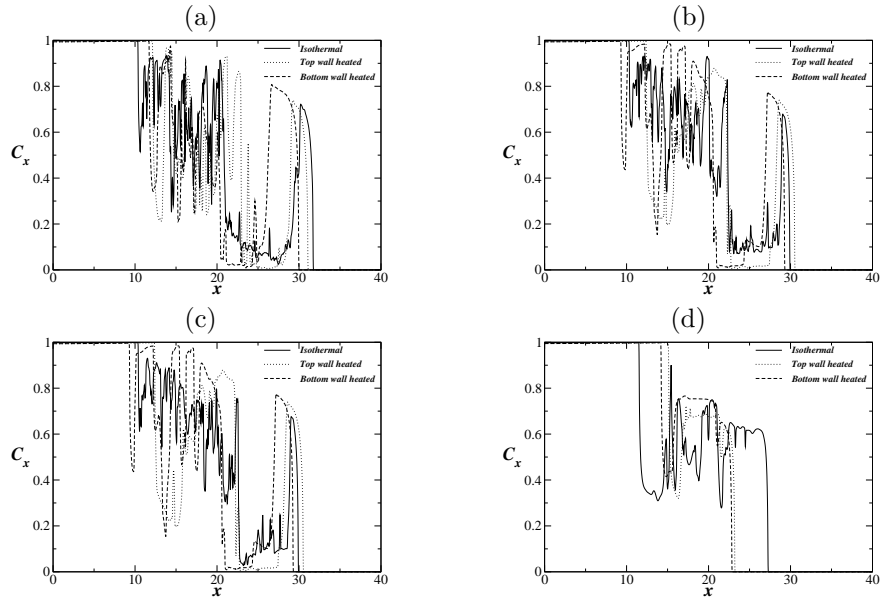
Figure 3.17: Effect of viscosity ratio on axial variation of depth-average C_x at t=100 as, (a)(b)(c)and(d)μ_r=0.01, 0.1, 1, 10
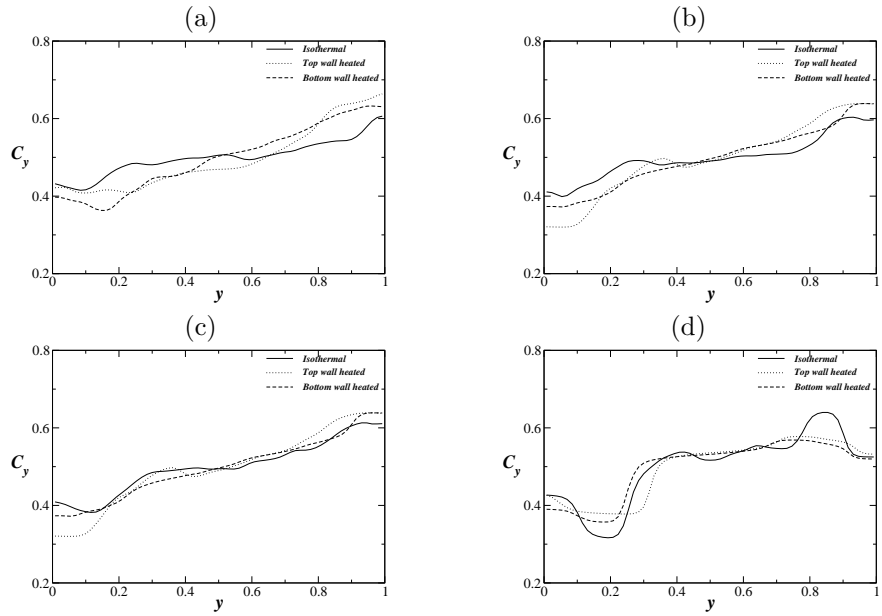
Figure 3.18: Effect of viscosity ratio on transverse variation of depth-average C_y at t=100, (a)(b)(c)and(d) as μ_r=0.01, 0.1, 1, 10

We investigate the effect of viscosity ratio. The contours of the volume fraction of the lighter fluid, C for μ_r=0.01, 0.1, 1, and 10 are ploted in Fig. [3.15-3.16] at 100 respectively.It is to be noted here that $\mu_r < 1$ ($\mu_r > 1$) represents the system where the heavier fluid is less (high) viscous. It can be seen that increasing viscosity ratio has a stabilizing influence. A similar finding was also observed by in case of pressure-driven flow in an inclined channel. It can also be seen that for $\mu_r \leq 1$ blob of lighter fluid is detached from the main finger of the lighter fluid and moves independently. However, the dynamics is not observed for $\mu_r \geq 1$. The speed of the fingers is much lesser than that of the isothermal case for μ_r=10. Fig. [3.17-3.18] shows the axial and transverse variation of viscosity varying from μ_r=0.01, 0.1, 1, and 10. Oscillation were reducing as viscosity ratio increased it implies stability increased. In this case the flow structure becomes more like two individual Poiseuille flow and two stable fingers of the lighter and heavier fluids propagate in the upward and download directions, respectively.

3.6   Effect of Marangoni number and density ratio

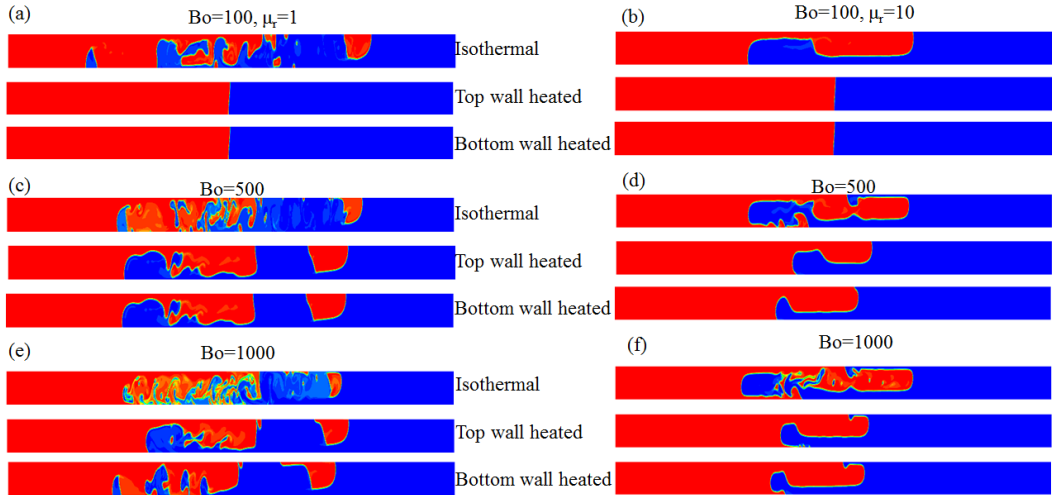Figure 3.19: Comparison of different Marangoni number and density Ratio obtained by finite volume(FV) method using 2562 and 66 grid points in x and y direction respectively, for channel of aspect ratio 1:40 at t=100
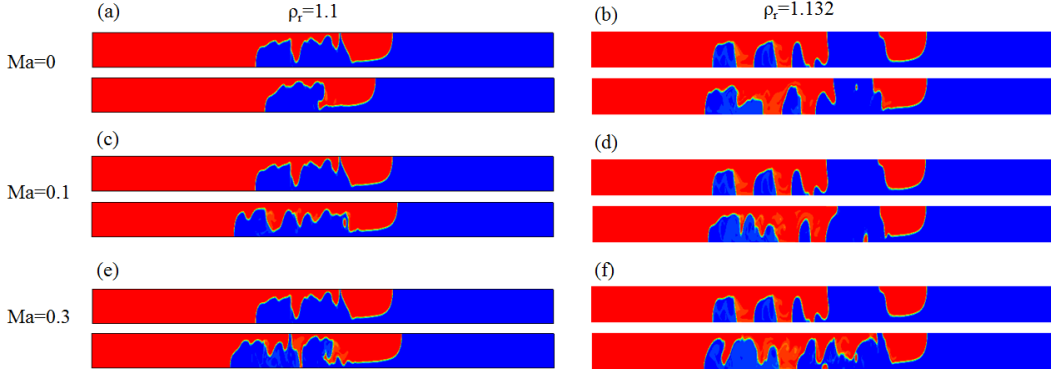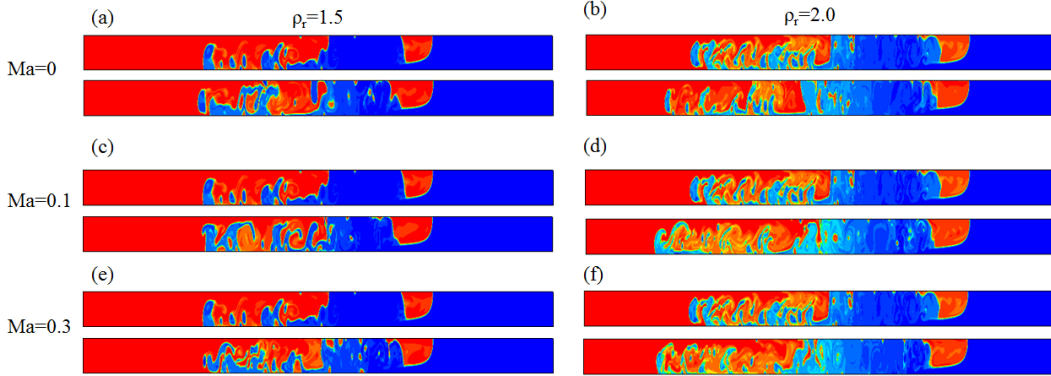

Figure 3.20: Comparison of different Marangoni number and density Ratio obtained by finite volume(FV) method using 2562 and 66 grid points in x and y direction respectively, for channel of aspect ratio 1:40 at t=50

Finally we have investigated the effects of Marangoni number and density ratio in Fig. [3.19-3.20] where the contours of the volume fraction of the lighter fluid, C are plotted for isothermal case, for different values of Ma=0, 0.1, and 0.3 and density ratio varying as 1.1, 1.132, 1.5 and 2. All the results presented are correspond to the configuration when the bottom wall is heated. It can be seen that increasing the value of the Marangoni number slightly increases the speed of the propagating fingers and also increases the intensity of the instabilities and thereby increases the 'mixing' efficiency of the fluids. It can also be observed that increasing the density ratio increases the spreading for all the cases.This is expected because the speed of the fingers depends on the local density contrast across the interface. For density ratio, ρ_r=2.0 it can be observed that the flow dynamics is completely dominated by the formation of the vortical structures which in turn give rise to intense 'mixing' of the fluids.

Chapter 4

Conclusions

The buoyancy-driven interpenetration of two immiscible fluids in a differentially heated inclined channel has been investigated numerically. The effects of Reynolds number, Bond number, Marangoni number, density ratio, viscosity ratio and temperature difference between the walls (ΔT) have been reported. The following conclusions are derived from the investigations presented in this thesis.

- Interfacial instability which is mixture of Kelvin-Helmholtz (KH) and Rayleigh-Taylor (RT) type instabilities have been observed due to motion of heavier and lighter fluids in the opposite direction.

- The flow dynamics and instability patterns in non-isothermal systems are very different as compared to those obtained in isothermal systems.

- The intensity of interfacial instabilities is very less as compared to those in isothermal case for $\text{Re} \leq 200$. This is due to thermal convection which acts to stabilize the flow.

- The bottom wall heated case is more unstable than the top wall heated for $\text{Re} \leq 200$ due to natural convection.

- The interfacial instability increases with increasing Reynolds number for both the isothermal and non-isothermal cases.

- Intensity of instabilities increases with increasing the wall temperature. This is due to increase in buoyancy force.

- Decreasing bond number (increasing surface tension) decreases the instability.

- The critical bond number is observed to be 100 for the set of parameter values considered below which there is no instability.

- For the fixed set of parameter values, increasing viscosity ratio decreases the intensity of the instabilities.

- Increasing Marangoni number increases the intensity of instabilities. This effect is significant for higher density ratio.

- Increasing density ratio also increases the formation of vortical structures due to increase in buoyancy force.

References

[1] T. B. Benjamin. Gravity currents and related phenomena. *J. Fluid Mech.* 31, (1968) 209-248.

[2] D. D. Joseph, R. Bai, K. P. Chen, and Y. Y. Renardy. Core-annular flows. *Ann. Rev. Fluid Mech.* 29, (1997) 65-90.

[3] M. Debacq, J-P. Hulin, D. Salin, B. Perrin and E. J. Hinch. Buoyant mixing of miscible fluids of varying viscosities in vertical tubes. *Phys. Fluids* 15 (12), (2003) 3846–3855.

[4] H. Ding, P. D. M. Spelt, and C. Shu. Diffuse interface model for incompressible two-phase flows with large density ratios. *J. Comput. Phys* 226, (2007) 2078–2095.

[5] K. C. Sahu and S. P. Vanka. A Multiphase Lattice Boltzmann Study of Buoyancy-Induced Mixing in a Tilted Channel *Computers & Fluids* 50, (2011) 199–215.

[6] P. R. Redapangu, S. P. Vanka, and K. C. Sahu. Multiphase lattice Boltzmann simulations of buoyancy-induced flow of two immiscible fluids with different viscosities. *European Journal of Mechanics B/Fluids* 34, (2012) 105–114.

[7] T. Séon and J. Znaien and B. Perrin and E. J. Hinch and D. Salin and J. P. Hulin. Front dynamics and macroscopic diffusion in buoyant mixing in a tilted tube. *Phys. Fluids* 19 (12), (2007) 125105.

[8] T. Séon and D. Salin and J. P. Hulin and E. J. Hinch and B. Perrin. Transient buoyancy-driven front dynamics in nearly horizontal tubes. *Phys. Fluids* 19, (2007) 123603.

[9] Y. Hallez and J. Magnaudet. Effects of channel geometry on buoyancy-driven mixing. *Phys. Fluids* 20, (2008) 053306.

[10] M. H. I. Baird, K. Aravamudan, N. V. R. Rao, J. Chadam, and A. P. Pierce. Unsteady axial mixing by natural convection in a vertical column. *AIChE J.* 38, (1992) 1825.

[11] T. Séon and D. Salin and J. P. Hulin and B. Perrin and E. J. Hinch. Buoyant mixing of miscible fluids in tilted tubes. *Phys. Fluids* 16, (2004) L103-L106.

[12] T. Séon and D. Salin and J. P. Hulin and B. Perrin and E. J. Hinch. Buoyancy driven miscible front dynamics in tilted tubes. *Phys. Fluids* 17, (2005) 031702.

[13] T. Séon and J. P. Hulin and D. Salin and B. Perrin and E. J. Hinch. From turbulent mixing to gravity currents in tilted tubes. *Phys. Fluids* 18, (2006) 091103.

[14] T. Séon and J. P. Hulin and D. Salin and B. Perrin and E. J. Hinch. Laser-induced fluorescence measurements of buoyancy driven mixing in tilted tubes. *Phys. Fluids* 18, (2006) 041701.

[15] M. M. Nasr-Azadani, , and E. Meiburg. Turbidity currents interacting with three-dimensional topography. *J. Fluid Mech.* 745, (2014) 409–443.

[16] M. M. Nasr-Azadani, B. Hall, and E. Meiburg. Polydisperse Turbidity Currents Propagating over Complex Topography: Comparison of Experimental and Depth-Resolved Simulation Results. *Comp. & Geosc.* 53, (2013) 141–153.

[17] A. Prakash and J. N. Koster. Steady natural convection in a two-layer system of immiscible liquids *International Journal of Heat and Mass Transfer* 40, (1997) 2799–2812.

[18] Q. S. Liu, B. Roux, and M. G. Velarde. Thermocapillary convection in two-layer systems. *International Journal of Heat and Mass Transfer* 41, (1998) 1499–1511.

[19] D. Villers and J. K. Platten. Thermal convection in superposed immiscible liquid layers. *Applied Scientific Research* 45, (1988) 145–152.

[20] A. Watson. The effect of the inversion temperature on the convection of water in an enclosed rectangular cavity. *Mechanical and Applied Math* 25, (1977) 423–446.

[21] M. A. Hossain and D. a. S. Rees. Natural convection flow of water near its density maximum in a rectangular enclosure having isothermal walls with heat generation *Heat and Mass Transfer* 41, (2005) 367–374.

[22] J. N. Koster and K. Y. Nguyen. Steady natural convection in a double layer of immiscible liquids with density inversion *International Journal of Heat and Mass Transfer* 39, (1996) 467–478.

[23] J. Fernandez, P. Kurowski, P. Petitjeans, and E. Meiburg. Density-driven unstable flows of miscible fluids in a Hele-Shaw cell *J. Fluid Mech.* 451, 239–260.

[24] T. Son, J.-P. Hulin, D. Salin, B. Perrin, and E. J. Hinch. Buoyant mixing of miscible fluids in tilted tubes *Phys. Fluids* 16, (2004) L103–L106.

[25] R. Balasubramaniam, N. Rashidnia, T. Maxworthy, and J. Kuang. Instability of miscible interfaces in a cylindrical tube *Phys. Fluids* 17, 052103.

[26] K. C. Sahu and S. P. Vanka. A multiphase lattice Boltzmann study of buoyancy-induced mixing in a tilted channel *Comp. & Fluids.* 50, 199–215.

[27] R. K. P. Wang. Transient Buoyancy-Thermocapillary Convection in Two Superposed Immiscible Liquid Layers. *Numerical Heat Transfer Part A-applications - NUMER HEAT TRANSFER PT A-APPL* 30, (1996) 477–501.

[28] R. W. Zeren and W. C. Reynolds. Thermal instabilities in two-fluid horizontal layers. *J. Fluid Mech.* 53, (1972) 305-327.

[29] Q. Chang and J. I. D. Alexander. Study of Marangoni-natural convection in a two-layer liquid system with density inversion using a lattice Boltzmann model. *Phys. Fluids* 19, (2007) 102107.

[30] P. R. Redapangu, K. Chandra Sahu, and S. P. Vanka. A Lattice Boltzmann Simulation of Three-Dimensional Displacement Flow of Two Immiscible Liquids in a Square Duct. *Journal of Fluids Engineering* 135, (2013) 121,202–121,202.

[31] K. C. Sahu. Double diffusive effects on pressure-driven miscible channel flow: Influence of variable diffusivity. *International Journal of Multiphase Flow* 55, (2013) 24–31.

[32] H. Ding, P. D. M. Spelt, and C. Shu. Diffuse interface model for incompressible two-phase flows with large density ratios. *Journal of Computational Physics* 226, (2007) 2078–2095.

[33] P. H. Oosthuizen, D. N. P. D.), and D. Naylor. An Introduction to Convective Heat Transfer Analysis. WCB/McGraw Hill, 1999.